《原子核物理评论》
www.npr.ac.cn Nuclear Physics Review
Started in 1984

$3M_{\odot}$ AGB星中^{26}Al核合成的网络计算和反应率灵敏度分析

高日梅　童雅阁　吴开谡

The Network Calculation of ^{26}Al Nucleosynthesis in 3M AGB Stars and the Sensitivity Analysis of Nuclear Reaction Rates

GAO Rimei, TONG Yage, WU Kaisu

在线阅读 View online: https://doi.org/10.11804/NuclPhysRev.38.2020065

引用格式:
高日梅, 童雅阁, 吴开谡. $3M_{\odot}$ AGB星中^{26}Al核合成的网络计算和反应率灵敏度分析[J]. 原子核物理评论, 2021, 38(1):1−7. doi: 10.11804/NuclPhysRev.38.2020065
GAO Rimei, TONG Yage, WU Kaisu. The Network Calculation of ^{26}Al Nucleosynthesis in $3M_{\odot}$ AGB Stars and the Sensitivity Analysis of Nuclear Reaction Rates[J]. Nuclear Physics Review, 2021, 38(1):1−7. doi: 10.11804/NuclPhysRev.38.2020065

第 38 卷 第 1 期 原 子 核 物 理 评 论 Vol. 38, No. 1
2021 年 3 月 Nuclear Physics Review Mar., 2021

Article ID: 1007-4627(2021)01–0001–07

The Network Calculation of ^{26}Al Nucleosynthesis in $3M_{\odot}$ AGB Stars and the Sensitivity Analysis of Nuclear Reaction Rates

GAO Rimei, TONG Yage, WU Kaisu†

(*School of Mathematics and Physics, Beijing University of Chemical Technology, Beijing 100029, China*)

Abstract: The network calculation of ^{26}Al nucleosynthesis in $3\,M_{\odot}$ AGB stars and the sensitivity analysis of nuclear reaction rates have been investigated in this article. After establishing a complete nuclear reaction network from carbon to silicon, combined with the latest nuclear reaction rate data, we have calculated the abundance of ^{26}Al. The results show that ^{26}Al is effectively synthesized in the AGB stars at the beginning, but as the reaction proceeding, ^{26}Al is consumed by a series of nuclear reactions. The MgAl cycle appears in the network of ^{26}Al. We divide the main nuclear reactions in the reaction network into three categories (n,γ), (p,γ) and (α,γ), and the sensitivity of nuclear reaction rates has been analyzed in detail. We have identified the most influential reactions in each type of nuclear reactions, they are: $^{25}\mathrm{Mg}(\mathrm{n},\gamma)^{26}\mathrm{Mg}$, $^{25}\mathrm{Mg}(\mathrm{p},\gamma)^{26}\mathrm{Al}$, $^{26}\mathrm{Mg}(\mathrm{p},\gamma)^{27}\mathrm{Al}$, $^{21}\mathrm{Ne}(\mathrm{p},\gamma)^{22}\mathrm{Na}$, $^{18}\mathrm{O}(\alpha,\gamma)^{22}\mathrm{Ne}$ and $^{22}\mathrm{Ne}(\alpha,\gamma)^{26}\mathrm{Mg}$. Among all the nuclear reactions involved in the present network, $^{25}\mathrm{Mg}(\mathrm{p},\gamma)^{26}\mathrm{Al}$ is the one that has the greatest impact on the yield of ^{26}Al, which deserves the attention of nuclear experimentalists.

Key words: ^{26}Al abundance; AGB stars; nuclear reaction network; sensitivity analysis

CLC number: O571.53 **Document code:** A **DOI:** 10.11804/NuclPhysRev.38.2020065

1 Introduction

In 1982, Mahoney *et al.*[1] discovered the γ rays with an energy of 1.809 MeV in the interstellar space due to the decay of ^{26}Al. ^{26}Al is an unstable nucleus (with a half-life of about 7.2×10^5 a), which decays into the excited states of ^{26}Mg by β^+ decay or electron capture, and a 1 809 MeV γ ray is emitted during the deexcitation process of the first 2^+ state of ^{26}Mg. So, by detecting the flux of this γ ray, the abundance of ^{26}Al in the interstellar can be reckoned[2]. Based on astronomical observations, Diehl *et al.*[3] estimated that the abundance of ^{26}Al in the interstellar is $(2.8\pm0.8)M_{\odot}$. The origin of such a large amount of aluminum has attracted widespread attention[4] and become an open problem in nuclear astrophysics.

According to the theoretical studies of nuclear astrophysics, the abundance of interstellar aluminum is mainly contributed by the nucleosynthesis in the following sites, type II supernovae[5–6], AGB stars[7–8], nova[9–12], Wolf–Rayet stars[13], and low energy heavy cosmic rays[14–15]. It is worth noting that Peng *et al.*[16–17] proposed an alternative way of nucleosynthesis for ^{26}Al from both SNII and SNI$_a$. The Gamma-Ray Imaging Spectrometer(GRIS) data indicate that AGB stars are a non-negligible site. Two evidences support that AGB stars play an important role in the origin of interstellar ^{26}Al. The first one, the high ^{26}Al/^{27}Al ratios observed in the silicon carbide(SiC) grains around the majority of AGB stars[18]. The second one, circumstellar spectroscopy observed the ^{26}Al around the nearest carbon star IRC+10216[19].

The nucleosynthesis study of AGB stars shows that ^{26}Al is synthesized at the bottom of the H combustion shell of the AGB stars(Hot Bottom Burning, referred to as HBB) through the NeNa cycle and the MgAl cycle[4]. Therefore, Mowlavi and Meynet[7] proposed that AGB stars might also be the main contributor to the interstellar ^{26}Al. They gave a detailed research on the production and destruction process of ^{26}Al in AGB stars and found that at the HBB of massive ($M>4M_{\odot}$) AGB stars a large amount of ^{26}Al could be synthesized, so HBB is likely to be the main site for the synthesis of ^{26}Al. In addition, according to Wasserburg *et al.*[20], AGB stars with initial mass $M=1.5\sim3M_{\odot}$ can also effectively synthes-

Received date: 18 Sep. 2020; **Revised date:** 29 Sep. 2020

Foundation item: Excellent Course Project of Beijing University of Chemical Technology(00810220)

Biography: GAO Rimei(1994–), female, Shuozhou, Shanxi Province, Student, Research interests: Differential Equations and Nuclear Astrophysics; E-mail: 18235193317@163.com

† **Corresponding author:** WU Kaisu, E-mail: wuks@mail.buct.edu.cn.

ize ^{26}Al. Due to the existence of divergence and the update of nuclear reaction rates, it is necessary to reanalyze and calculate the nucleosynthesis of ^{26}Al in AGB stars, which is also one of the main purposes of this article. Another main purpose of this article is to analyze the sensitivity of the nuclear reaction rates associated with ^{26}Al nucleosynthesis, and to identify which nuclear reactions having more impact on the yield of ^{26}Al. It should be pointed out that the sensitivity of the nuclear reactions relevant to the ^{26}Al nucleosynthesis in the stage of explosive neon–carbon burning in the massive stars has been systematically studied by Iliadis *et al.*[21]. In this work, we focus on the steady combustion stage of the $3\,M_{\odot}$ AGB stars.

This paper studies the nucleosynthesis of ^{26}Al and the sensitivity of related nuclear reactions in $3\,M_{\odot}$ AGB stars. In order to calculate the abundance of ^{26}Al, first of all, an entire reaction network from carbon to silicon isotopes is constructed. This reaction network contains 25 nuclides and 102 nuclear reactions ranging from ^{12}C to ^{40}Si. Furthermore, a related nuclear reaction network equation system is established, which is a highly stiff differential equation system[22], and the coefficient of the network equations is the reaction rates of nuclear reactions. Using the semi-implicit Runge-Kutan method[23], we establish the relevant calculation program and give the numerical solution of the network equations. Our calculation results show that ^{26}Al can be effectively synthesized and subsequently consumed by a series of nuclear reactions in AGB stars, and reaction flow calculations show that the MgAl cycle has a positive effect on the synthesis of ^{26}Al. Then, the main nuclear reactions involved in the nucleosynthesis of ^{26}Al are divided into three types, namely (n,γ), (p,γ) and (α,γ), and the sensitivity analysis of the reaction rates of these nuclear reactions is carried out in detail by using our calculation program. With the variable-controlling approach, the reaction rate of one nuclear reaction is changed from $-20\,\%$ to 20% each time, with each step increasing by 5%. By changing the step once, the corresponding differential equations can be solved to obtain the ^{26}Al abundance variation curve. We define sensitivity as the sum of the product of the function value of the ^{26}Al abundance curve node and the step length of the differential equation system. In fact, this definition of sensitivity is equivalent to the Euclidean norm of the function. Therefore, the sensitivity of the corresponding curve after changing the step length can be obtained, and the sensitivity change curve can be obtained. In this way, we have identified the most influential reactions and they are: ^{25}Mg$(\mathrm{n},\gamma)^{26}$Mg, ^{25}Mg$(\mathrm{p},\gamma)^{26}$Al, ^{26}Mg$(\mathrm{p},\gamma)^{27}$Al, ^{21}Ne$(\mathrm{p},\gamma)^{22}$Na, ^{18}O$(\alpha,\gamma)^{22}$Ne and ^{22}Ne$(\alpha,\gamma)^{26}$Mg. Among all reactions, ^{25}Mg$(\mathrm{p},\gamma)^{26}$Al is the reaction that has the greatest impact on the yield of ^{26}Al.

This paper is organized as follows. In Section 2, models and a nuclear reaction network are set up. In Section 3, the evolution chart of various nuclides and the MgAl cycle flow graph are presented. Section 4 concentrates on reaction rate sensitivity for the three types of nuclear reactions (n,γ), (p,γ) and (α,γ). The nuclear reactions having the large influence upon ^{26}Al abundance are distinguished. A summary and some conclusions are made at the end.

2 Model and method

2.1 Establishment of nuclear reaction network

The nuclear reaction(Fig. 1 for details) network contains 25 nuclides from ^{12}C to ^{40}Si and 102 nuclear reactions. The latest nuclear reactions and nuclear structure data come from the JINA Reaclib Database and CINA Database. All the data in the two databases are ongoing updates, publicly available and can be downloaded via web. The former is maintained by the Joint Institute for Nuclear Astrophysics(http://groups.nscl.msu.edu/jina/reaclib/db/), the latter is managed by the Computational Infrastructure for Nuclear Astrophysics(http://www.nucastrodata.org).

2.2 Nuclear reaction equations

The various nuclear reactions in the stellar interior arouse chemical composition variation in the reaction zone, which is followed by the structural changes of pressure, temperature, density, and so on. Therefore, the fundamental cause of the stellar evolution is thermonuclear reactions. Unquestionably, it is crucial to investigate the variation of chemical composition, resulting from nuclear reactions, for the research of the evolution of the structure inside the stars. Assuming in the volume of $1\,\mathrm{cm}^3$ per second, the number of the element i particle varies as follows:

$$\frac{\mathrm{d}n_i}{\mathrm{d}t} = -\sum_j \frac{a_i}{1+\delta_{ij}} r_{ij}(m) + \sum_{k,l} \frac{b_i}{1+\delta_{kl}} r_{kl}(i),$$
$$\delta_{ij} = \begin{cases} 0, & i \neq j \\ 1, & i = j, \end{cases} \quad \delta_{kl} = \begin{cases} 0, & k \neq l \\ 1, & k = l, \end{cases} \tag{1}$$

where $r_{ij}(m)$ is the total number of nuclear reactions in which i target nuclides interact with j incident particles to generate m particles. In other words, the total number of i particles consumes in $1\,\mathrm{cm}^3$ volume per second. $r_{kl}(i)$ is similar to $r_{ij}(m)$, $r_{kl}(i)$ represents generation. In Eq. (1), a_i denotes the number of particles involving and consuming in a nuclear reac-

^{12}C(n, γ)^{13}C	^{15}N(p, α)^{12}C	^{18}F(β$^+$)^{18}O	^{22}Na(β$^+$)^{22}Ne	^{26}Mg(n, γ)^{27}Mg(β$^-$)^{27}Al
^{12}C(p, γ)^{13}N	^{15}N(p, γ)^{16}O	^{18}F(n, γ)^{19}F	^{22}Na(n, α)^{19}F	^{26}Al(n, p)^{26}Mg
^{12}C(α, γ)^{16}O	^{15}N(α, γ)^{19}F	^{19}F(n, γ)^{20}F(β$^-$)^{20}Ne	^{22}Na(n, γ)^{23}Na	^{26}Al(n, α)^{23}Na
^{13}C(n, γ)^{14}C	^{16}O(n, γ)^{17}O	^{19}F(p, α)^{16}O	^{22}Na(α, γ)^{26}Al	^{26}Al(β$^+$)^{26}Mg
^{13}C(p, γ)^{14}N	^{16}O(p, γ)^{17}F(β$^+$)^{17}O	^{19}F(p, γ)^{20}Ne	^{22}Na(α, p)^{25}Mg	^{26}Al(n, γ)^{27}Al
^{13}C(α, n)^{16}O	^{16}O(α, γ)^{20}Ne	^{19}F(α, p)^{22}Ne	^{23}Na(p, α)^{20}Ne	^{26}Al(α, γ)^{30}P(ε)^{30}Si
^{14}C(n, γ)^{15}C(β$^-$)^{15}N	^{17}O(n, α)^{14}C	^{19}F(α, γ)^{23}Na	^{23}Na(p, γ)^{24}Mg	^{26}Al(α, p)^{29}Si
^{14}C(p, γ)^{15}N	^{17}O(n, γ)^{18}O	^{20}Ne(n, γ)^{21}Ne	^{23}Na(n, γ)^{24}Na	^{27}Al(p, γ)^{28}Si
^{14}C(α, γ)^{18}O	^{17}O(p, α)^{14}N	^{20}Ne(p, γ)^{21}Na(β$^+$)^{21}Ne	^{23}Na(α, γ)^{27}Al	^{27}Al(p, α)^{24}Mg
^{14}C(β$^-$)^{14}N	^{17}O(p, γ)^{18}F	^{20}Ne(α, γ)^{24}Mg	^{23}Na(α, p)^{26}Mg	^{27}Al(n, γ)^{28}Al(β$^-$)^{28}Si
^{14}C(p, n)^{14}N	^{17}O(α, γ)^{21}Ne	^{21}Ne(n, γ)^{22}Ne	^{24}Mg(n, γ)^{25}Mg	^{27}Al(α, γ)^{31}P
^{13}N(n, p)^{13}C	^{17}O(α, n)^{20}Ne	^{21}Ne(p, γ)^{22}Na	^{24}Mg(α, γ)^{28}Si	^{27}Al(α, p)^{30}Si
^{13}N(p, γ)^{14}O(β$^+$)^{14}N	^{18}O(n, γ)^{19}O(β$^-$)^{19}F	^{21}Ne(α, n)^{24}Mg	^{25}Mg(p, γ)^{26}Al	^{28}Si(n, γ)^{29}Si
^{13}N(α, p)^{16}O	^{18}O(p, α)^{15}N	^{21}Ne(n, α)^{18}O	^{25}Mg(α, γ)^{29}Si	^{28}Si(α, γ)^{32}S
^{13}N(β$^+$)^{13}C	^{18}O(p, γ)^{19}F	^{22}Ne(p, γ)^{23}Na	^{25}Mg(α, n)^{28}Si	^{29}Si(n, γ)^{30}Si
^{13}N(n, γ)^{14}N	^{18}O(α, γ)^{22}Ne	^{22}Ne(n, γ)^{23}Ne(β$^-$)^{23}Na	^{25}Mg(n, γ)^{26}Mg	^{29}Si(p, γ)^{30}P(ε)^{30}Si
^{14}N(n, γ)^{15}N	^{18}O(α, n)^{21}Ne	^{22}Ne(α, γ)^{26}Mg	^{25}Mg(n, α)^{22}Ne	^{29}Si(α, γ)^{33}S
^{14}N(n, p)^{14}C	^{18}F(n, α)^{15}N	^{22}Ne(α, n)^{25}Mg	^{26}Mg(p, γ)^{27}Al	^{30}Si(p, γ)^{31}P
^{14}N(p, γ)^{15}O	^{18}F(n, p)^{18}O	^{22}Na(n, p)^{22}Ne	^{26}Mg(α, γ)^{30}Si	^{30}Si(n, γ)^{31}Si
^{14}N(α, γ)^{18}F	^{18}F(p, α)^{15}O	^{22}Na(p, γ)^{23}Mg(β$^+$)^{23}Na	^{26}Mg(α, n)^{29}Si	^{30}Si(α, γ)^{34}S
^{15}N(n, γ)^{16}N(β$^-$)^{16}O	^{18}F(α, p)^{21}Ne			

Fig. 1　Nuclear reaction network.
Note: JINA Reaclib Database and CINA Database.

tion, and similar to a_i, b_i denotes production. By introducting a new variable, $Y_i = X_i/A_i$, where Y_i is the element abundance, the particles density can be written as:

$$n_i = \frac{\rho X_i}{A_i} N_A = \rho N_A Y_i, \tag{2}$$

where, ρ, X_i, N_A and A_i are density, elemental mass fraction, Avogadro constant and the atomic weight of the element, respectively. In Eq. (1), $r_{ij}(m)$ and $r_{kl}(i)$ can be expressed as follows:

$$r_{ij}(m) = n_i n_j \langle \sigma\nu \rangle_{ij}, \quad r_{kl}(i) = n_k n_l \langle \sigma\nu \rangle_{kl}, \tag{3}$$

where, $\langle \sigma\nu \rangle_{ij}$ denotes the nuclear reaction rate of i particles and j particles. Combining Eq. (2) and Eq. (3), Eq. (1) can be expressed as:

$$\begin{aligned} \frac{\mathrm{d}Y_i}{\mathrm{d}t} =& -\rho N_A \sum_j \frac{a_i}{1+\delta_{ij}} Y_i Y_j \langle \sigma\nu \rangle_{ij} + \\ & \rho N_A \sum_{k,l} \frac{b_i}{1+\delta_{kl}} Y_k Y_l \langle \sigma\nu \rangle_{kl}. \end{aligned} \tag{4}$$

Here, $a_i = b_i = 1$ and $\delta_{ij} = \delta_{kl} = 0$. The abundance of $^4_2$He particles is almost unchanged in $3\,M_{\odot}$ AGB stars. Therefore, this Eq. (4) can be expressed as follows:

$$\begin{aligned} \frac{\mathrm{d}Y_j}{\mathrm{d}t} =& \rho Y_\alpha \sum (N_A \langle \sigma\nu \rangle_{i\alpha} Y_i - N_A \langle \sigma\nu \rangle_{j\alpha} Y_j) + \\ & \sum (Y_i \lambda_{ij} - Y_j \lambda_{ji}) + N_{\mathrm{n}} (\langle \sigma\nu \rangle_{in} Y_i - \\ & \langle \sigma\nu \rangle_{jn} Y_j) + N_{\mathrm{p}} (\langle \sigma\nu \rangle_{ip} Y_i - \langle \sigma\nu \rangle_{jp} Y_j), \end{aligned} \tag{5}$$

where, N_{n} and N_{p} are the density of neutrons and protons, respectively. In Eq. (5), each term represents the effect on nuclear reactions with α particles, $\beta^{\pm}$, the neutron and the proton.

2.3 Calculation method of nuclear reaction equations

All equations are established on the basis of the nuclear reaction network, in which the coefficient is the nuclear reaction rates. The attribute of equations, high stiffness, is determined by greatly different reaction rates' magnitude. The numerical solution of the semi-implicit Runge-Kuta method is as follows:

For a problem[24]:

$$\begin{cases} y' = f(t, y), \quad a \leqslant t \leqslant b \\ y(a) = \eta \end{cases}, \tag{6}$$

the numercial solution format can be determined by the following forms

$$\begin{aligned} y_{n+1} =& y_n + w_1 k_1 + w_2 k_2 \\ k_1 =& h[1 - h a_1 A(t_n, y_n)]^{-1} f(t_n, y_n) \\ k_2 =& h[1 - h a_2 A(t_n + c_2 h, y_n + c_{21} k_1)]^{-1} \times \\ & f(t_n + b_2 h, y_n + b_{21} k_1), \end{aligned}$$

where, h represents the step length. a, b, c, w are all coefficients, which have a lot of groups of values. The parameters are chosen here

$$a_1 = 1 + \frac{\sqrt{6}}{6} = 1.408\,248\,29,$$
$$a_2 = 1 - \frac{\sqrt{6}}{6} = 0.591\,751\,71,$$
$$b_{21} = c_{21} = \frac{-6 - \sqrt{6} + \sqrt{58 + 20\sqrt{6}}}{6 + 2\sqrt{6}} = 0.173\,786\,67,$$
$$b_2 = c_2 = 0.173\,786\,67,$$
$$w_1 = -0.413\,154\,32,$$
$$w_2 = 1.413\,154\,32.$$

Rosenbrock' s semi-implicit Runge-Kutta method, which avoids iteration and retains the stability of the calculation format, is chosen to solve the equations. It greatly improves the efficiency of code execution.

3 Numerical results

3.1 Initial conditions and determination of parameters

In HBB of $3\,M_\odot$ AGB stars, the key physical parameters are the density ρ=1 500 g/cm^3, the burning temperature T=3×10^8 K and the initial mole abundances of Y_0(^{4}He)=0.175 and Y_0(^{12}C)=0.014, and other relevant nuclide abundance values are given according to the Ref. [25]. The injection way of ^{13}C is gradual, which keeps neutron density stable[26]. In low-mass AGB stars, the neutron value is taken as n=10^7 cm^{-3} that is mainly from nuclear reactions ^{13}C(α,n)^{16}O and ^{18}O(α,n)^{21}Ne[27]. The proton source is included in the reaction network, especially the nuclear reactions ^{14}N(n,p)^{14}C and ^{26}Al(n,p)^{26}Mg.

Fig. 2 shows, the abundance of ^{19}F firstly increases over time due to the role of reaction ^{14}N(α, γ)^{19}F. The curve of ^{19}F quickly begins to decline because it primarily produces ^{22}Ne. It can be seen that the abundance curve of ^{25}Mg is stable at first, and then it increases mainly because of the ^{22}Ne(α,n)^{25}Mg reaction. The abundance curve of ^{26}Al gradually decreases via ^{26}Al(n,p)^{26}Mg and ^{26}Al(β^+)^{26}Mg, while the content of ^{26}Mg subsequently increases. ^{23}Na is the seed for the synthesis of ^{27}Al, so ^{27}Al nuclide abundance remains stable. ^{24}Mg abundance can also rise and form the MgAl cycle by the reaction ^{27}Al(p, α)^{24}Mg. Finally, the reduction of raw materials leads the ^{26}Al consumption more than production, and its abundance decreases rapidly.

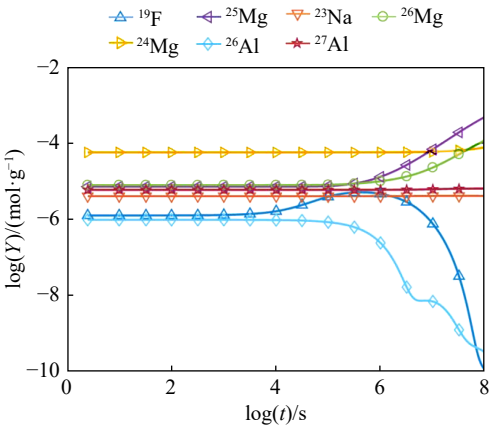

Fig. 2 (color online) The abundances of various nuclides evolving over the time.

3.2 The existence of the MgAl cycle

The nuclear reaction network equations describe the dynamic changes of each nuclide in the network. By calculating the reaction flow between two nuclides, we can see the dynamic changes between the various nuclides more clearly.

For two nuclides, the reaction flow is defined as follows:

$$F_{ij}(t) = \int_0^t [Y_i(i \to j)]\mathrm{d}t, \tag{7}$$

where, F_{ij} denotes reaction flow, and $Y_i(i \to j)$ is the abundance of nuclide i converted to nuclide j. The entire time span is integrated to find the main path for the synthesis of ^{26}Al. Within $10^8 s$, the flow chart of the MgAl cycle is shown in Fig. 3.

As shown in Fig. 3, the MgAl cycle is presented as ^{24}Mg(n, γ)^{25}Mg(p, γ)^{26}Al(β^+)^{26}Mg(p, γ)^{27}Al(p, α)^{24}Mg.

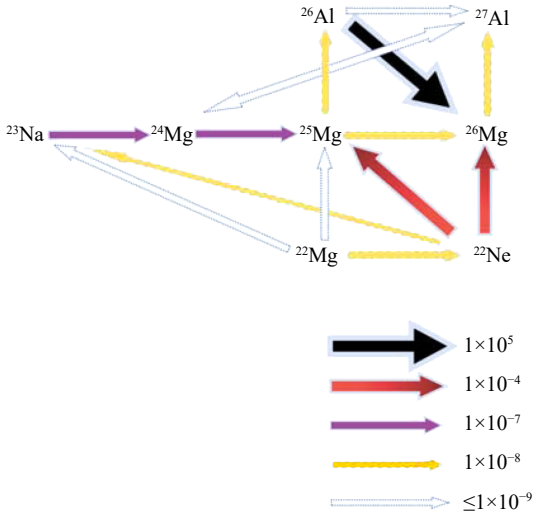

Fig. 3 (color online) The calculated the MgAl cycle reaction flow.

4 Sensitive analysis

In the nuclear reaction network equations, the decisive factor is the reaction rates. The reaction rates determine the yield of each nuclide and the direction

of reaction flow. The reaction rates can be obtained by experiments or by theoretical models if the experimental data are scarce. Whether it is experimental measurements or theoretical estimations, there are certain errors in the rates. Therefore, sensitivity analysis of the reaction rates in the network is very important, especially through sensitivity analysis, we can find out nuclear reactions that have a relatively large impact on the abundance of ^{26}Al. This can help the experimentalists to choose the important reactions which need more precise measurements. As for sensitivity calculation, under the variable-controlling approach, only the rate of one nuclear reaction is altered from –20% to 20%, increasing by 5% per time for eight times to measure the sensitivity of ^{26}Al. By drawing, the impact of each nuclear reaction on ^{26}Al abundance can be compared intuitively. Expression of the sensitivity metric is as follows:

$$D^2 = \sum (F - F^0)^2 \cdot h, \tag{8}$$

where, D represents the sensitivity metric; F^0 is the ^{26}Al abundance from the original reaction rate; F is the ^{26}Al abundance with varying the reaction rate; h is the step size. To compare the sensitivity of each nuclear reaction more clearly, the y-coordinate sensitivity measure D is logarithm base 10 and the x-coordinate is –20%~20%, increasing by 5% each time. The sensitivity analysis for three types of nuclear reactions (n, γ), (p, γ) and (α, γ) is studied. The results are presented Fig. 4~7 as showing below.

4.1 (n, γ) sensitivity analysis

Fig. 4 shows that ^{25}Mg(n, γ)^{26}Mg has the greatest impact on the synthesis of ^{26}Al and ^{26}Al(n, γ)^{27}Al takes the second place. Compared with other nuclear reactions, the impact of ^{25}Mg(n, γ)^{26}Mg on ^{26}Al is larger at least one order of magnitude than that of the other (n, γ) reactions. Among all the (n, γ) reactions, the sensitivity of ^{26}Al(n, γ)^{27}Al is in second place. Thus, it can be considered that ^{26}Al(n, γ)^{27}Al is one of the main nuclear reactions for consuming ^{26}Al.

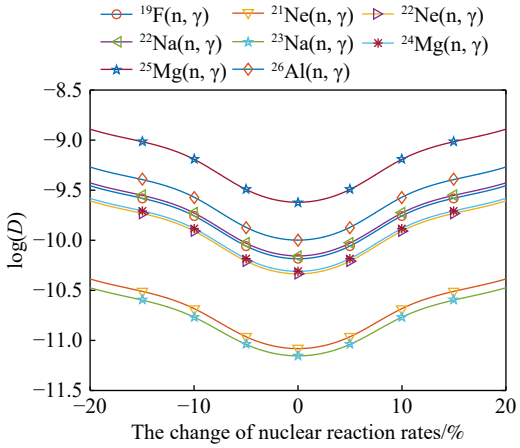

Fig. 4 (color online) (n, γ) sensitivity analysis. Only eight reactions are shown, and the remaining sensitivities are too small to show in the Fig. 4 (Similar to Fig. 5 and Fig. 6)

4.2 (p, γ) sensitivity analysis

Fig. 5 shows that the sensitivity of ^{25}Mg(p, γ)^{26}Al is the largest. It is found that the production of ^{25}Mg(p, γ)^{26}Al to ^{26}Al is at least five orders of magnitude higher than ^{22}Na(α, γ)^{26}Al. The secondary important reactions are ^{26}Mg(p, γ)^{27}Al, ^{21}Ne(p, γ)^{22}Na, ^{22}Ne(p, γ)^{23}Na, ^{12}C(p, γ)^{13}N and ^{16}O(p, γ)^{17}F(β^+)^{17}O. Thereinto, ^{25}Mg(p, γ)^{26}Al should be the prime target for future measurement.

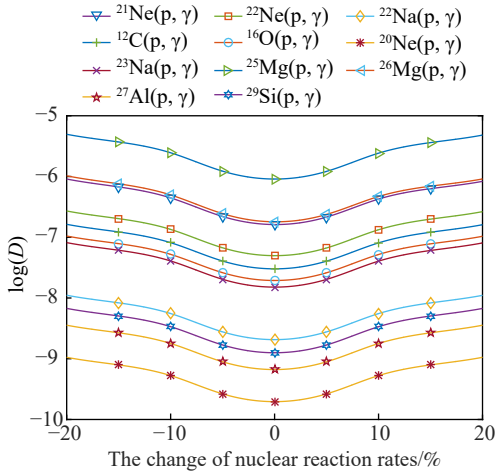

Fig. 5 (color online) (p, γ) sensitivity analysis

4.3 (α, γ) sensitivity analysis

Fig. 6 shows that, in the type of (α, γ), the nuclear reactions that have a relatively large impact on ^{26}Al are ^{18}O(α, γ)^{22}Ne, ^{22}Ne(α, γ)^{26}Mg, ^{15}N(α, γ)^{19}F and ^{19}F(α, γ)^{23}Na.

Finally, in order to obtain the overall impact of the three types of nuclear reactions on the yield of ^{26}Al, we select several reactions with higher sensitivity in each type of reaction, and show in Fig. 7.

Fig. 7 shows that among all the three types of nuclear reactions, ^{25}Mg(p, γ)^{26}Al is the one that has the greatest impact on the yield of ^{26}Al. Therefore, we recommend that nuclear experimentalists pay more attention to it.

5 Summary and conclusions

In $3M_{\odot}$ AGB stars, the network calculation of ^{26}Al nucleosynthesis and the sensitivity analysis of nuclear reaction data have been given. Firstly, we build a complete reaction network from carbon to sil-

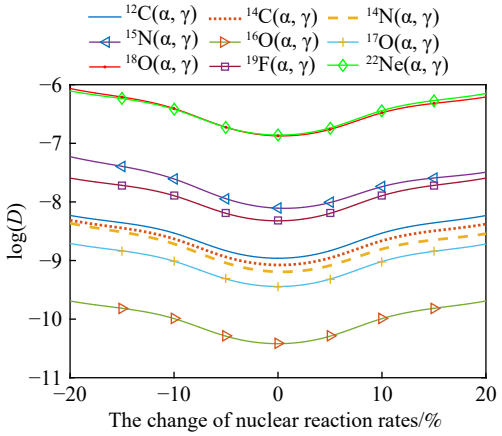

Fig. 6 (color online) (α, γ) sensitivity analysis.

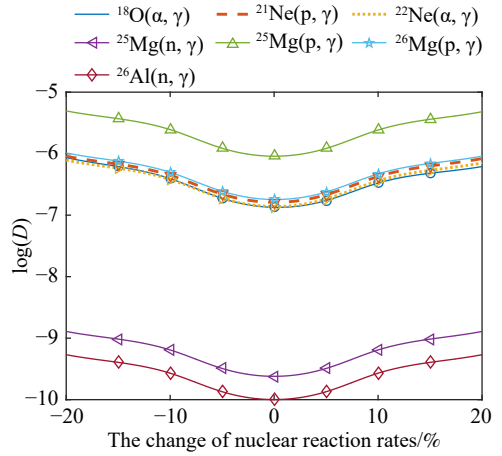

Fig. 7 (color online) Comparison of three types of nuclear reaction sensitivity.

icon combing with the latest nuclear reaction rates. As the nuclear reactions proceed, the nucleosynthesis of ^{26}Al is computed in detail, and the calculation of the reaction flow shows the existence of the MgAl cycle. Furthermore, we also analyze the sensitivity of three reaction types (n, γ), (p, γ) and (α, γ) to the production of ^{26}Al. The result indicates: the reaction rates of ^{25}Mg(n, γ)^{26}Mg, ^{25}Mg(p, γ)^{26}Al, ^{26}Mg(p, γ)^{27}Al, ^{21}Ne(p, γ)^{22}Na, ^{18}O(α, γ)^{22}Ne and ^{22}Ne(α, γ)^{26}Mg have the greatest impact on the nucleosynthesis of ^{26}Al. In particular, the ^{25}Mg(p, γ)^{26}Al reaction is the most important reaction of all, further experimental studies of this reaction are recommended.

Acknowledgments This work is supported by the Excellent Course Project of Beijing University of Chemical Technology. The author sincerely thanks the anonymous reviewers for their excellent reviews and their valuable comments.

References:

[1] MAHONEY W A, LING J C, JACOBSON A S, et al. The Astrophysical Journal, 1982, 262: 742.
[2] DIEHL R, TIMMES F X. Publications of the Astronomical Society of the Pacific, 1998, 110(748): 637.
[3] DIEHL R, HALLOIN H, KRETSCHMER K, et al. Nature, 2006, 439(7072): 45.
[4] LIU Honglin, LUO Zhiquan. Nuclear Physics Review, 2008, 25(1): 31. (in Chinese)
(刘宏林, 罗志全. 原子核物理评论, 2008, 25(1): 31.)
[5] FUJIMOTO Y, KRUMHOLZ M R, INUTSUKA S. Monthly Notices of the Royal Astronomical Society, 2020, 497(2): 2442.
[6] TIMMES F X, WOOSLEY S E, HARTMANN D H, et al. Astrophysical Journal, 1995, 449: 204.
[7] MOWLAVI N, MEYNET G. Astronomy and Astrophysics, 2000, 361(3): 959.
[8] FORESTINI M, CHARBONNEL C. Astronomy and Astrophysics Supplement Series, 1997, 123: 241.
[9] JOSÉ J, HERNANZ M, COC A. The Astrophysical Journal, 1997, 479(1): L55.
[10] KOLB U, POLITANO M. Astronomy and Astrophysics, 1997, 319(3): 909.
[11] ARNOULD M, NORGAARD H, THIELEMANN F K, et al. The Astrophysical Journal, 1980, 237: 931.
[12] CLAYTON D D. The Astrophysical Journal, 1984, 280: 144.
[13] ARNOULD M, PAULUS G, MEYNET G. Astronomy Astrophysics, 1997, 321(2): 452.
[14] GACHES B A L, WALCH S, OFFNER S S R, et al. The Astrophysical Journal, 2020, 898(1): 79.
[15] CLAYTON D. Nature, 1994, 368: 222.
[16] WANG Peng, PENG Qiuhe, ZHANG Shuinai, et al. Chinese Physics Letters, 2006, 23(6): 1652.
[17] PENG Qiuhe. New Astronomy Reviews, 2006, 50(7): 481.
[18] CHERCHNEFF I, CAU P. Symposium-International Astronomical Union, 1999, 191: 251.
[19] GUELIN M, FORESTIN M, VALIRON P, et al. Astronomy and Astrophysics, 1995, 21(5): 321.
[20] WASSERBURG G J, BUSSO M, GALLINO R, et al. Nuclear Physics A, 2006, 777: 5.
[21] ILIADIS C, CHAMPAGNE A, CHIEFFI A, et al. The Astrophysical Journal Supplement Series, 2011, 193(1): 16.
[22] TIMMES F X, HOFFMAN R D, WOOSLEY S E. The Astrophysical Journal Supplement Series, 2000, 129(1): 377.
[23] ROSENBROCK H H. Computer Journal, 1963, 5(4): 329.
[24] YUAN Xinding. Numerical Solution of Initial Value Problem of Rigid Ordinary Differential Equation[M]. Beijing: Science Press, 1987: 341. (in Chinese).
(袁新鼎. 刚性常微分方程初值问题的数值解法[M]. 北京：科学出版社, 1987: 341.)
[25] FORESTINI M, GORIELY S, JORISSEN A, et al. Astronomy and Astrophysics, 1992, 261(1): 157.
[26] HOLLOWELL D, IBEN I J. The Astrophysical Journal, 1989, 340: 966.
[27] STRANIERO O, GALLINO R, BUSSO M, et al. The Astrophysical Journal Letters, 1995, 440: L85.

$3M_{\odot}$ AGB星中^{26}Al核合成的网络计算和反应率灵敏度分析

高日梅, 童雅阁, 吴开谡†

(北京化工大学数理学院，北京 100029)

摘要: 研究了$3\,M_{\odot}$AGB星中^{26}Al核合成的网络计算和核反应率的灵敏度分析。结合最新的核反应率数据，建立了一个从碳到硅完整的核反应网络，计算了^{26}Al的丰度。结果表明，^{26}Al首先在AGB星中有效合成，随着核反应的进行，然后被一系列的核反应消耗。MgAl循环出现在^{26}Al的网络中。我们将核反应网络中的主要核反应分为三类：(n,γ)，(p,γ)和(α,γ)，并对核反应率的灵敏度进行了详细的分析。已经确定了每一类中最有影响的核反应，它们是$^{25}\mathrm{Mg}(\mathrm{n},\gamma)^{26}\mathrm{Mg}$，$^{25}\mathrm{Mg}(\mathrm{p},\gamma)^{26}\mathrm{Al}$，$^{26}\mathrm{Mg}(\mathrm{p},\gamma)^{27}\mathrm{Al}$，$^{21}\mathrm{Ne}(\mathrm{p},\gamma)^{22}\mathrm{Na}$，$^{18}\mathrm{O}(\alpha,\gamma)^{22}\mathrm{Ne}$和$^{22}\mathrm{Ne}(\alpha,\gamma)^{26}\mathrm{Mg}$。在目前网络所涉及的所有核反应中，$^{25}\mathrm{Mg}(\mathrm{p},\gamma)^{26}\mathrm{Al}$是对^{26}Al的产量有最大的影响，它值得核实验物理学家的关注。

关键词: ^{26}Al丰度；AGB星；核反应网络；灵敏度分析

收稿日期: 2020-09-18；　**修改日期:** 2020-09-29

基金项目: 北京化工大学优秀课程项目（00810220）

† **通信作者:** 吴开谡，E-mail：wuks@mail.buct.edu.cn。